Modelling Damage in Nuclear Graphite

Thorsten Becker [1,*], **James Marrow**[2]

[1] Department of Mechanical and Mechatronic Engineering, Stellenbosch University, Stellenbosch 7600, South Africa
[2] Department of Materials, University of Oxford, Oxford OX1 3PH, United Kingdom
* Corresponding author: tbecker@sun.ac.za

Abstract In this paper a non-local coupled plasticity and damage model for nuclear graphite is presented. The model is the adaption of an existing model for quasi-brittle materials that allows for the degradation (as a function of load) of the material properties. The model arises from the continuum-based approach and uses concepts of isotropic damaged elasticity in combination with isotropic tensile and compressive plasticity to represent inelastic behaviour. In this work fracture of Gilsocarbon polygranular graphite is simulated in the FE environment for compact tension and three point bend specimens. The model consists of a combination of non-associated multi-hardening plasticity and scalar (isotropic) damage elasticity that describe the irreversible damage that occurs during the fracturing process in graphite. The simulations exhibit the observed softening and degradation of the material and found to be size and geometry independent.

Keywords Nuclear graphite, fracture mechanics, micro-cracking, non-local damage plasticity model.

1. Introduction

Nuclear graphite, a high purity grade polygranular graphite, is used for structural components as well as neutron moderators in high temperature nuclear reactors. Functionally, graphite components are arranged in the form of keyed bricks to accommodate the thermal and radiation induced deformations throughout the life of a reactor. Potentially, these dimensional changes may lead to stresses that are sufficient for crack initiation in the brittle graphite, particularly at keyway roots and other discontinuities. The structural integrity of such components is of importance, and has been assessed historically with either probability of failure methodologies (such as the Weibull approach) [1–4] or the fracture mechanics methodology [5–12].

Weibull's weakest link theory anticipates that the larger the volume of material the greater the chance that a defect exists within the volume [13]. Simple application of this theory is inconsistent with experimental results; failure predictions of graphite components from small specimens do not agree with those of larger specimens [14]. An adaptation to the Weibull approach has been proposed by Hindley et al. [1] which incorperates a fixed volume size to ensure size independence; however, the results have shown to be conservative [1].

Recent studies have shown graphite behaviour to be non-linear [15] for non-irradiated medium grained graphites (Gilsocarbon and NBG10). Crack propagation is associated with a fracture process zone (FPZ) in which extensive micro-cracking results in irreversable energy dissipation. One of the biggest challenges in predicting component failure in graphite when using conventional fracture mechanics is that the fracture process is influenced by the graphite's micro-, meso- and macrostructures, which are characterised by the number and distribution of internal pores and cracks [15]. For example, crack propagation in Gilsocarbon is primarily linked with damage initiation and propagation from these internal features. In a notched specimen under an increasing load, isolated and randomly distributed micro-cracks develop predominantly ahead of the notch tip and propagate orthogonally to the tensile strain in the loading direction. It is during this phase that damage accumulates; ultimately the micro-cracks coalesce into a macro-crack. The propagation of the macro-crack is accompanied by bridging or branching through the maze of micro flaws and is

preceded by a fracture process zone (FPZ) ahead of the crack tip. Therefore, fracture processes in graphite may depend primarily on the stability of the interfacial cracks (micro-cracks) which is a function of the material structure [6,15,16].

Becker et al. [15] has shown, using the Double Torsion geometry [17] and an algorithm to calculate the fracture parameters from digital image correlation obtained displacement fields [18], that:

- The LEFM fracture parameters G_{Ic} or K_{Ic} are dependent on specimen geometry and size.
- The non-linear contributions to the energy dissipated during fracture seem dependent on specimen geometry and size.
- *R*-curve behaviour seems dependent on specimen geometry and size.

However

- The elastic contributions to the energy dissipated during fracture appear to be independent of specimen geometry and size.

These mechanisms of fracture are not unique. Quasi-brittle materials, like concrete, rock and many other materials including various fiber composites and particulate composites, coarse-grained or toughened ceramics, ice, cemented sands, grouted soils, bone, paper, wood, wood-particle board, etc experience similar mechanism of fracture [19]. Such materials are generally considered as brittle, yet behave in a non-linear fashion due to the development of a sizable FPZ that can occupy a large portion of the structure and is believed to be geometry and size dependent [19].

One way to model quasi-brittle fracture is the use of a non-local damage plasticity model, such as proposed by Lubliner and coauthors [20] and Lee and Fenves [21]. Here, the behavior of micro cracking is modelled on a macroscopic level by stiffness degradation combined with plasticity to provide an appropriate evolution of a yield surface during the formation of damage. The model uses a fracture energy based scalar damage variable to represent the damage state. In addition to the damage variable, the model introduces elastic and plastic degradation variables to simulate the degradation of elastic stiffness.

This paper presents the utilisation of this non-local damage-plasticity (DP) model for quasi-brittle materials to simulate graphite fracture. The framework of the non-local DP model is presented and the calibration of the model parameters with experimental data for Gilsocarbon. Finally, the model is implemented using two different test geometry examples, namely a three point bend (3PB) geometry and two compact tension (CT) geometries.

2. Framework for plastic-damage model for nuclear graphite

The model simulates failure implicitly in the Finite Element (FE) environment and consists of a combination of non-associated multi-hardening plasticity and scalar (isotropic) damaged elasticity variables to describe the irreversible damage that occurs during the fracture. This requires the definition of a yield surface and a flow rule. The degradation mechanisms of tensile cracking and compressive crushing are defined respectively as G_f, the fracture energy, and as a stress-displacement hardening relationship in compression . The degradation of the elastic stiffness in tension and compression is defined as a scalar, which is a function of the cracking displacement or strain. As static conditions are simulated, a strain rate independent model is assumed. For details regarding the model derivation, the reader is referred to the papers by Lubliner [20] and Lee and Fenves [21].

The yield function takes the form of the Drucker and Prager yield criterion to account for different evolution of strength under tension and compression. The evolution of the yield surface is controlled by the two hardening variables ε_c^{pl} and ε_t^{pl}. In terms of effective stresses, the yield function takes the form [22]:

$$F = \frac{1}{1-\alpha}\left(\bar{p} - 3\alpha\bar{q} + \beta\varepsilon_t^{pl}\langle\hat{\bar{\sigma}}_{max}\rangle - \gamma\langle\hat{\bar{\sigma}}_{max}\rangle\right) - \hat{\bar{\sigma}}_c\varepsilon_c^{pl} \leq 0 \tag{1}$$

where, α, β and γ are dimensionless constants, $\langle\hat{\bar{\sigma}}_{max}\rangle$ is the algebraic maximum principal stress, $\bar{p}$ the hydrostatic pressure, which is a function of the first stress invariant I_1 (defined as $\bar{p} = I_1/3$), and $\bar{q}$ the Von Mises equivalent stress, described as $\bar{q} = \sqrt{2J_2}$ (where J_2 is the second deviatoric stress invariant). α, β and γ are given as:

$$\alpha = \frac{f_{b0}/f_{c0} - 1}{2f_{b0}/f_{c0} - 1} \tag{2}$$

$$\beta = \frac{f_{c0}}{f_{t0}}(\alpha - 1) - (1 + \alpha) \tag{3}$$

$$\gamma = \frac{3(1-\kappa_c)}{2\kappa_c - 1} \tag{4}$$

where, f_{c0} and f_{b0} are the compressive and compressive biaxial elastic limit respectively, f_{t0} the tensile elastic limit, and κ_c is the ratio of the second stress invariant on the tensile meridian to that on the compressive meridian at the elastic limit for any given value of the pressure invariant such that the maximum principal stress is negative (the default value is 2/3) [22].

To compute the non-elastic stress-strain behaviour, the plastic-damage model assumes non-associated potential flow as [22]:

$$\dot{\varepsilon}^{pl} = \lambda\frac{\partial G(\bar{\sigma})}{\partial\bar{\sigma}} \tag{5}$$

where the flow rule G is the Drucker-Prager hyperbolic function [22]:

$$G = \sqrt{(\epsilon_{cc}f_{t0}tan\psi)^2 + (\bar{q})^2} - \bar{p}tan\psi \tag{6}$$

where ϵ_{cc} is the eccentricity, which defines the rate at which the plastic potential function approaches the asymptote. ψ is the dilation angle (measured in the $\bar{p}$ - $\bar{q}$ plane at a high confining pressure.

The post-yield behaviour in tension is defined according to the energy criterion G_f. Quasi-brittle behaviour is characterised by a stress-displacement response and the fracture energy is invoked by specifying the post-yield stress as a function of cracking displacement. The tensile damage is converted to a cracking displacement value using a relationship where the specimen length l is assumed to be one unit length in FE implementation [22]. The post-yield behaviour in compression is defined as a displacement-hardening/softening behaviour. A cracking displacement u_c^{ck} is defined as the total displacement minus the elastic displacement corresponding to the undamaged material. This requires the softening data in terms of the cracking displacement [22]:

$$u_t^{pl} = u_t^{ck} - \frac{1}{1-d_t}\frac{\sigma_t l}{E_0} \tag{7}$$

3. Identification of the model parameters

The nuclear graphite grade modelled was Gilsocarbon (GCMB grade, IG-110) graphite, a near isotropic material [23]. Typical material properties are reported as 11.9 GPa for the Young's modulus and the tensile strength of 20 MPa [23]. The Poisson's ratio was taken as 0.21 [23]. The numerical strategy for solving the non-local DP problem requires the knowledge of the constitutive material parameters of Gilsocarbon, which include the definition of the yield surface, the flow rule, the load response and the material degradation.

3.1. Yield Surface and Flow Rule

The plane stress cross section for the failure surface in the principal stress space is shown in Figure 1a. The data shown was extracted from various literature sources on the biaxial behaviour of Gislocarbon (which have been listed in the captions for convenience). The typical uniaxial compressive yield stress to biaxial yield compressive stress ratio was found to be 0.81 [24]. The dilatancy and eccentricity values, ψ and the ϵ_{cc} respectivly, were extracted from Brocklehurst [2,25] as shown in Figure 1b. The dilation angle, measured in the p - q plane at high confining pressure, was calculated as 30°. Note, similar values were found for concrete, a quasi-brittle material, where ψ is between 30° to 40° [26]. Figure 1 shows that the Ducker-Prager criterion is an excellent fit to the failure data. Since a plane stress problem is assumed the triaxial parameter λ is of little significance [21].

3.2. Stiffness Degradation

The tension softening behaviour or post-yield behaviour is defined according to the fracture energy criterion $G_{f,}$ which is approximately 250 J/m² [15] for Gilsocarbon. To determine the stiffness degradation behaviour requires a complex testing apparatus, such as the tests done by Gopalaratnam and Shah [27] for concrete. At point in time when this work was undertaken these data were not available and thus a linear evolution of the damage variable with efffective plastic displacement is currently assumed. This ensures that when the effective plastic displacement reaches a critical value, the material stiffness will be fully degraded. The compressive load response was defined according to Oku [28]. The stiffness degradation behaviour was also defined as a linear evolution of the damage variable with effective plastic displacement. As static conditions are simulated a strain rate independent model is assumed. The parameters are summarised in Table 1.

Table 1: Material parameters of the DP model for Gilsocarbon

Elastic Properties:	
Young's modulus E_0	11.9 GPa
Poisson's ratio v	0.21
Yield Surface and Flow Rule:	
Dilation angle ψ	30°
Eccentricity ϵ_{cc}	4.8
Biaxiality ratio	0.81
Tension softening:	
Fracture energy	250 J/m^2
Compression hardening:	
20 MPa	0 mm
65 MPa	0.015 mm
1 MPa	0.045 mm

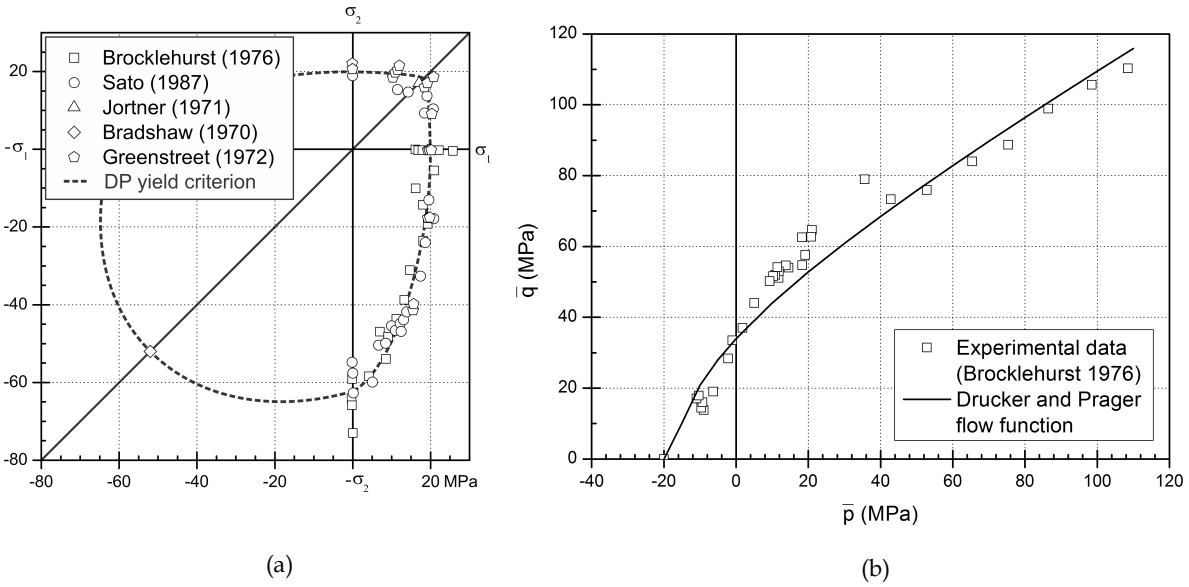

(a) (b)

Figure 1: (a) Biaxial failure data for Gislocarbon. The data was extracted from Brocklehurst [2], Sato et al. [29], Jortner [30], Bradshaw [24] and Greenstreet [31]. (b) Drucker-Prager hyperbolic plastic potential function in the meridional plane. Experimental data was extracted from Brocklehurst [2].

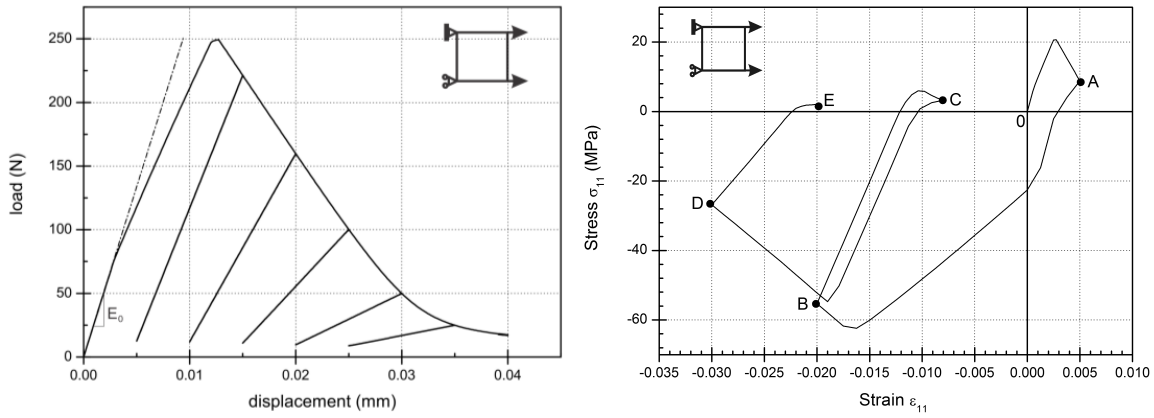

Figure 2: (a) Numerical solution of cyclic uniaxial loading in tension. (b) Numerical Solution for Full Cyclic Loading (Path: O-A-B-C-D-E).

3.3. Model Behaviour

To present the behaviour of the DP model a single monotonic uni-axial loading and full cyclic monotonic uni-axial loading element is simulated. This uses a linear elastic quadratic full integration element. The material properties used for each model are presented in Table 1. The element mesh size of 7.4 x 7.4 mm was utilised, as it represents the by Bazant et al. [32] defined characteristic length of Gislocarbon [33]. The model was implemented in the FE environment of ABAQUS/Standard (Version 6.9).

The non-local DP model monotonic uni-axial loading response, in Figure 2a, shows the softening response and the stiffness degradation (damage formation). The full cyclic (tension and compression) monotonic uni-axial loading response, in Figure 2b, resembles the hysteresis curve of

the simulation results in Figure 2a, because energy is dissipated during the tensile reloading (path B-C-D). Similar to Lee and Fenves [21], Figure 2 shows that the model can simulate quasi-brittle material behaviour subjected to cyclic loading for which the hysteresis curve in the tensile region is negligible compared with the compressive counterpart.

4. Numerical Implementation

The non-local DP model was implemented using two different Gislocarbon test geometry examples, namely a three point bend (3PB) gemetry and two compact tension (CT) geometries. Plane stress conditions were assumed to allow for short computational times and numerical convergence. The computations were implemented in ABAQUS/Standard (Version 6.9). The material properties used for each model are presented in Table 1.

The first example is the two CT specimens tested by Fazluddin [8] and Hodgkins [7]. Note, for Hodgkins' specimen configuration the width of part of the specimen was reduced in order to allow the progression of the crack to be monitored in three dimensions using X- Ray tomography [7]. The numerical models consisted of 1480 and 1320 four noded plane strain elements for Fazluddin's and Hodgkins' geometries respectively (which only represent the symmetrical half). The second example, 3PB specimen, consists of 896 four noded linear plane strain elements and similarly only represents the symmetrical half of the specimen. To avoid convergence issues, only DP elements are utilised in the region in which fracture is expected to occur (elsewhere linear elastic conditions are assumed). Some mesh refinement was performed in the vicinity of the notch-tip to achieve mesh-insensitive results. Boundary conditions are applied with an analytically rigid pin with defined hard frictionless contact in displacement control.

The failure envelope is well captured in both the CT specimens and the 3PB specimen. The tensile damage localisation at peak load, which manifests itself by a reduction of the load at fracture, shows similarities to the experimental observations reported by Becker et al. [15]. The experimental data from Hodgkins provided a load-unloading response (Figure 3b) and the non-local DP model is capable, to a certain degree, of simulating this behaviour. Discrepencies exist as some load carrying capability remains in fully degraded elements since the stress-displacement behaviour has been defined with a failure stress of 1 MPa for numerical stability [22]. The 3PB geometry exhibits a more brittle response compared to the CT geometry, which is noticeable from the more severe post peak load drop when comparing Figure 3 and Figure 4.

It is worth reiterrating that experimentally obtained R-curve data has shown a geometry dependent fracture behavior of Gilsocarbon, where the non-linearities due to the FPZ and the wake effects result in variations of the apparent fracture toughness [15]. Since the DP model is a non-local approach it is size and geometry independent. The degradation and hence softening of the material is confined to the defined yield criteria and flow rule. As damage develops ahead of the crack tip, the yield surface shrinks in the stress space leading to a softening interfacial constitutive law. Fracture has occurred when the work done by the tractions meets the fracture mechanics based criterion. The DP failure model can be viewed as an extension or generalisation of the cohesive zone model proposed by Zou et al. [34], in that it couples together the effects of stress/displacement curves to derive a combined non-local stress and fracture mechanics based failure criterion. Because the DP model is non-local it is not confined to stress singularities and is thus believed to be a more accurate representation of graphite fracture.

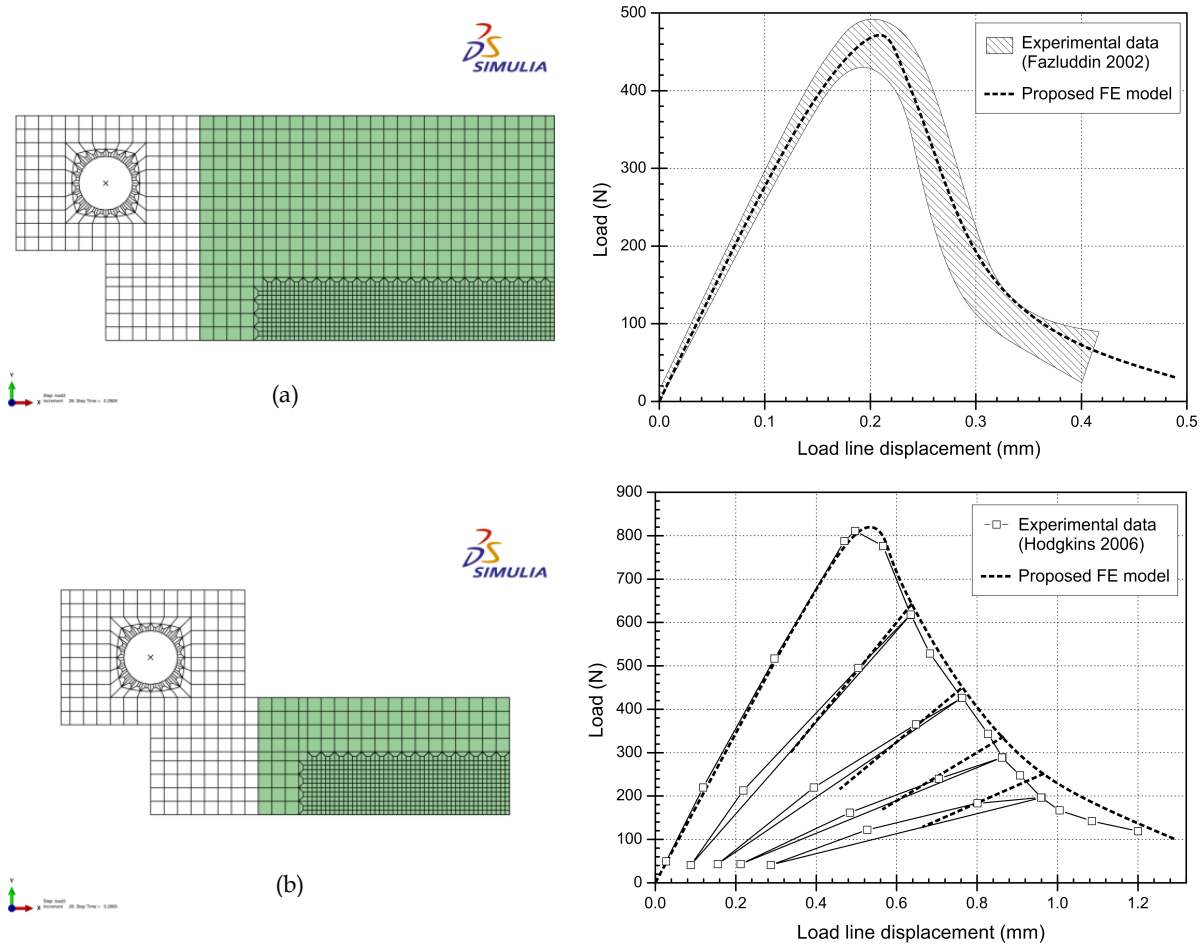

Figure 3: FE mesh of the two DP simulated CT specimens: (a) according Fazluddin's CT specimen [8] with W = 50 mm and the load displacement curves. (b) according Hodgkins' CT specimen [7] with W = 87 mm and the load displacement curves. Coloured elements indicate DP elements.

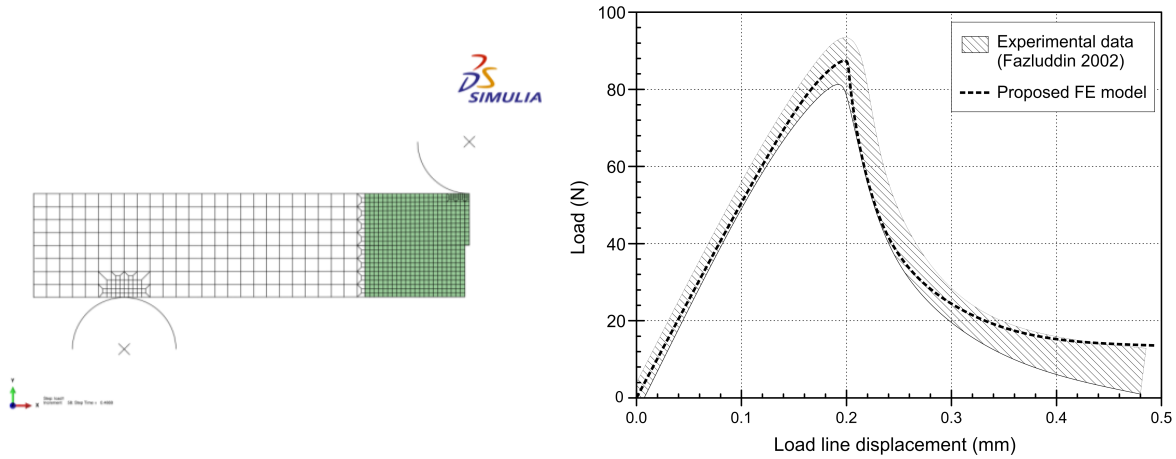

Figure 4: Fazluddin's geometry and loading setup of the three point bending simulation [8] and load-displacement curve. Coloured elements indicate DP elements.

5. Conclusion

The non-local DP model is a useful methodology in the rate-independent, non-linear modelling of fracture in Gilsocarbon. The significance of the result is both theoretical and practical: On the theoretical plane, though the conventional EPFM methodology has been shown to be limited in the application in nuclear graphite, it was demonstrated that the fracture parameters calculated using EPFM are relevant as they describe the inherent failure behviour. Since the model allows for the bulk degradation of material ahead of the crack tip, fracture is not constrained to a singularity, but is simulated as the degradation of the material ahead of the crack tip. The practical significance is that the DP model has shown excellent agreement with experimental results and hence motivates for further investigations of using non local DP models to simulate quasi-brittle fracture in nuclear graphite that has been degraded by operation in reactor environments.

Acknowledgments

TH Becker would like to express his appreciation for the University of Cape Town and the people involved in facilitating this research and to the University of Manchester for providing the required experimental equipment, such as the mechanical testing apparatuses as well as for the use of the server cluster.

References

[1] M.P. Hindley, M.N. Mitchell, C. Erasmus, R. McMurtry, T.H. Becker, D.C. Blaine, A.A. Groenwold, Journal of Nuclear Materials, Available online 30 October 2012, ISSN 0022-3115, 10.1016/j.jnucmat.2012.10.030.
[2] J. Brocklehurst, M. Darby, Materials Science and Engineering 16 (1974) 91–106.
[3] B. Mitchell, J. Smart, S. Fok, B. Marsden, Journal of Nuclear Materials 322 (2003) 126–137.
[4] J.P. Strizak, IAEA-TECDOC-690 (Ed.), 1991, p. 16.
[5] P. Ouagne, G.B. Neighbour, B. McEnaney, Journal of Physics D: Applied Physics 35 (2002) 927–934.
[6] A. Hodgkins, T. Marrow, P. Mummery, B. Marsden, A. Fok, Materials Science and Technology 22 (2006) 1051.
[7] A.D. Hodgkin, Crack Propagation in Nuclear Graphite, PhD Thesis, The University of Manchester, 2006.
[8] S. Fazluddin, Crack Growth Resistance in Nuclear Graphite, University of Sheffield, 2002.
[9] M. Sakai, K. Urashima, M. Inagaki, Journal of the American Ceramic Society 66 (1983) 868–874.
[10] M. Sakai, J. Yoshimura, Y. Goto, M. Inagaki, Journal of the American Ceramic Society 71 (1988) 609–616.
[11] M.R. Ayatollahi, a. R. Torabi, Carbon 48 (2010) 2255–2265.
[12] P.J. Heard, M.R. Wootton, R. Moskovic, P.E.J. Flewitt, Journal of Nuclear Materials 401 (2010) 71–77.
[13] W. Weibull, Roy. Swedish Ins. Eng. Res. 153 (n.d.) 1–55.
[14] M.P. Hindley, M.N. Mitchell, D.C. Blaine, A.A. Groenwold, Journal of Nuclear Materials 420 (2012) 110–115.
[15] T.H. Becker, T.J. Marrow, R.B. Tait, Journal of Nuclear Materials 414 (2011) 32–43.
[16] M. Mostafavi, T.J. Marrow, Engineering Fracture Mechanics 78 (2011) 1756–1770.
[17] T.H. Becker, T.J. Marrow, R.B. Tait, Experimental Mechanics 51 (2011) 1511–1526.

[18] T.H. Becker, M. Mostafavi, T.J. Marrow, Fatigue and Fracture of Engineering Materials and Structures 35 (2012) 971–984.
[19] Z. Bazant, Engineering Fracture Mechanics 69 (2002) 165–205.
[20] J. Lubliner, International Journal of Solids and Structures 25 (1989) 299–326.
[21] J. Lee, G.L. Fenves, Journal of Engineering Mechanics 124 (1998) 892.
[22] ABAQUS, User's Manual, Version 6.9, ABAQUS Inc., Prvidence, Rhode Island, 2010.
[23] S.D. Preston, B.J. Marsden, Carbon 44 (2006) 1250–1257.
[24] W.G. Bradshaw, Mechanical and Thermal Properties of Glass-like Carbons, Technical Report CONF-701105 (1972).
[25] C. Berre, P. Mummery, B. Marsden, T. Mori, P.J. Withers, Journal of Nuclear Materials 381 (2008) 128.
[26] R. Malm, Predicting Shear Type Crack Initiation and Growth in Concrete with Non-linear Finite Element Method, Royal Institute of Technology (KTH), Stockholm, Sweden, 2009.
[27] V. Gopalaratnam, S. Shah, Journal Proceedings 82 (1985) -323.
[28] T. Oku, M. Eto, Nuclear Engineering and Design 143 (1993) 239–243.
[29] S. Sata, Nuclear Engineering and Design 23 (1987) 62.
[30] J. Jortner, Technical Report AFML-TR-71 (1971) 253.
[31] W. Greenstreet, G. Yahr, R. Valachovic, Carbon 11 (1973) -57.
[32] Z. Bazant, Advanced Cement Based Materials 4 (1996) 128–137.
[33] T.H. Becker, Understanding and Modelling the Damage and Fracture Characteristics of Nuclear Grade Graphite, PhD Thesis, University of Cape Town, 2011.
[34] Z. Zou, Journal of Nuclear Materials 324 (2004) 116–124.